DOI: 10.53375/ijecer.2023.331

JOURNAL OF ELECTRICAL AND COMPUTER ENGINEERING RESEARCH
VOL. 3, NO. 1, 2023

Comparison Between Different Droop Based Control Techniques and a Virtual Control Oscillator

Carlos G. C. Branco[1,*], Jordi El Mariachet Carreno[1], Mingshen Li[1], Francisco Kleber de A. Lima[2], José Matas[1], Josep M. Guerrero[3]
[1] Electrical Engineering Department, Politechnic University of Catalonia, Spain,
Email: carlos.gustavo.castelo@upc.edu, jorge.el.mariachet@upc.edu, mingshen.li@upc.edu, jose.matas@upc.edu
[2]Electrical Engineering Department, Federal University of Ceara, Brazil,
Email: kleber@ufc.br
[3]Energy Teknik Department, Aalborg University, Denmark,
Email: joz@energy.aau.dk
[*] *Corresponding author*

Abstract: **This work presents a literature review about control techniques for parallel connected power inverters under microgrid applications. Some control strategies, based on droop control for parallel inverters of distributed generation units in an ac distribution system will be presented in this work. Finally, an important method called Virtual Oscillating Control (VOC) is suggested for connecting voltage source inverters. Inverters are able to work in parallel with a constant-voltage constant frequency system, as well as with other inverters and also in standalone operation. The different power sources can share the load also under unbalanced conditions. Throughout this work several simulation results are presented in order to demonstrate the behaviour the behavior of the different control strategies tested.**

Keywords: **Microgrids, Virtual Oscillating Control, Droop Control, Paralleled Inverters, Virtual Impedance.**

I. INTRODUCTION

Uninterruptible Power Supplies (UPS) are equipments used to provide continuous power supply of high quality to critical systems or subsystems, increasing the availability and reliability of supply to levels much higher than those originally found in utility networks However, like all electronic equipment, the UPS is also prone to failure.

A possibility to improve the reliability of the UPS circuits it's the use of redundancy techniques. UPS redundancy can be accomplished by connecting the outputs of different UPS directly in parallel, which may bring advantages as: increasing in both reliability and power capacity of the system.

The parallelism without communication presents a greater level of reliability, but its implementation is more complex, when compared with the case where there is communication and centralized control, because each UPS has no information about the power flows of the other equipments.

The authors would like to thank the financial support from Postgraduate Support Program (PROAP) maintained by the Coordination for the Improvement of Higher Level Personnel (CAPES).

Thus, it becomes necessary to employ a control law, such that, based only on measurements of local variables, the load power will be distributed among the units equally or proportionally to the individual capacities of each unit.

It is possible to carry out the parallelism of the UPS systems without communication through the method called Droop control [1-3].

This method imposes a reduction in the amplitude of the voltage output of the UPS in accordance with the growth of reactive power supplied and a frequency reduction of output voltage in accordance with growth of the active power supplied.

II. DROOP CONTROL LOOP

The droop control originally is based on the power flow relations between voltage sources connected to a common bus. If the line connecting both has a mainly inductive characteristic, then these relations are described in (1) and (2) when they are part of a sentence, as in

$$P = \frac{E \cdot V}{X} \sin \phi \quad (1)$$

$$Q = \frac{E \cdot V \cdot \cos \phi - V^2}{X} \quad (2)$$

where E is the voltage source amplitude, V the bus voltage, X the line reactance, P and Q active and reactive powers, respectively.

The classical droop method states that since P is mostly dependant of the angle and Q of the amplitude E, they can be controlled in a closed-loop fashion by (3) and (4)

$$\omega = \omega^* - m \cdot P \quad (3)$$

$$E = E^{*} - n \cdot Q \tag{4}$$

A. dq Rotating Reference Frame Transformation

Assuming the two orthogonal sinusoidal state variables given by (5) and (6)

$$X_R = X \cdot \cos(\omega t + \varphi) \tag{5}$$

$$X_I = X \cdot \sin(\omega t + \varphi) \tag{6}$$

where X is the amplitude, ω is the fundamental frequency and φ is the initial phase.

Then, the dq frame state variables are related to the variables of time frame by (7)

$$\begin{bmatrix} X_d \\ X_q \end{bmatrix} = T \cdot \begin{bmatrix} X_R \\ X_I \end{bmatrix} \tag{7}$$

where

$$T = \begin{bmatrix} \cos(\omega t) & \sin(\omega t) \\ -\sin(\omega t) & \cos(\omega t) \end{bmatrix} \tag{8}$$

III. DROOP CONTROL WITH VIRTUAL IMPEDANCE LOOP AND IMPROVED PERFORMANCE

Droop control, despite its capability of load sharing between UPS's without control communication, presents a major draw- back that must be overcome, that is its compromise between proper power sharing accuracy and good amplitude and frequency output voltage regulation [1]. On [2] it is proposed a control scheme based on a Virtual Output Impedance concept and a modified Droop Control technique to obtain a faster transient response and more power sharing accuracy. Also, the voltage regulation loop is based on a modified PID controller.

A. Voltage Regulation Loop

Instead of using a PID controller, the regulation is realized via a modified PID. The utility of this more complex controller is to provide a better and more reliable transient response to the system, in comparison to the classical one [2].

$$\begin{aligned} & L \cdot C \frac{\partial^2 \langle \upsilon_o \rangle}{\partial t} + r_L \cdot C \frac{\partial \langle \upsilon_o \rangle}{\partial t} + \langle \upsilon_o \rangle \\ & + L \frac{\partial \langle i_o \rangle}{\partial t} + r_L \langle i_o \rangle = \langle k \cdot V_{in} \rangle \end{aligned} \tag{9}$$

where k varies according to the type of modulation used, for three-level, $k = \{-1, 0, 1\}$; for two-level, $k = \{-1, 1\}$.

The proposed controller, gives the relation between the error ($\upsilon_{ref} - \upsilon_o$) and the modulation signal

$$\begin{aligned} \langle k \cdot V_{in} \rangle &= \upsilon_{ref} + k_p(\upsilon_{ref} - \langle \upsilon_0 \rangle) \\ & + k_i \int (\upsilon_{ref} - \langle \upsilon_0 \rangle) \\ & + k_d \frac{\partial}{\partial t}(\upsilon_{ref} - \langle \upsilon_0 \rangle) \end{aligned} \tag{10}$$

When (9) is put into (10) the result is the closed-loop Thévenin model of the inverter, given by (11)

$$\upsilon_0 = G(s) \cdot \upsilon_{ref} - Z_0(s) \cdot i_0 \tag{11}$$

The Bode diagrams for G(s) and Zo(s) are shown in the following figures.

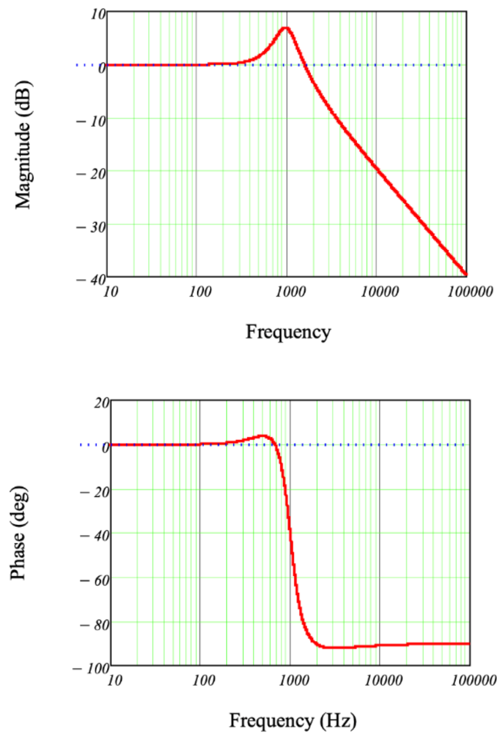

Fig. 1. G(s) Bode diagram: Magnitude (above) and phase (below).

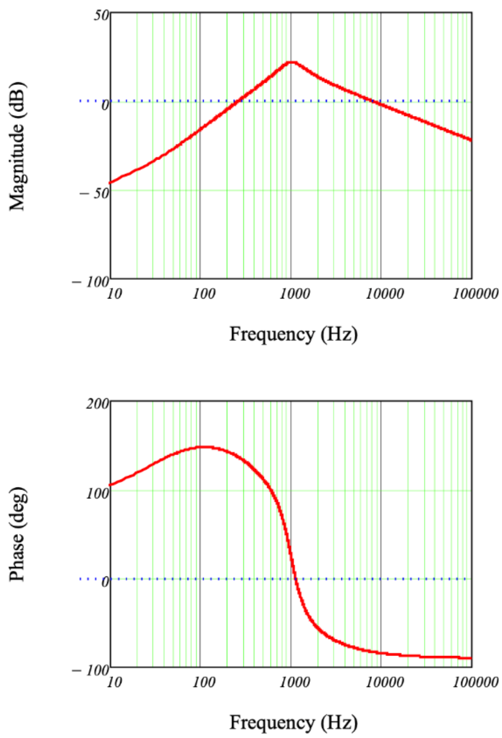

Fig. 2. Z_o(s) Bode diagram: magnitude (above) and phase (below).

B. Virtual Impedance Concept

With the objective of imposing the wanted inductive line characteristic, some authors adopt a bulky inductor externally connected to the inverter [4,5].

Another way to achieve this is to add in the control scheme a Virtual Output Impedance, which will be computational load to the system, but will be a cheaper and lighter solution.

The Virtual Impedance proposed by [6] let's the system present an inductive behavior at low frequencies and a resistive behavior at high frequencies, improving the inverter's voltage THD under non-linear loads, which is given by (12).

The UPS output impedance, also called Thévenin Impedance, is a function of the output filter, considering its inductor, capacitor and their equivalent resistances, and of the output voltage regulator's parameters.

This output impedance, composed with the proposed controller, possesses highly resistive characteristics, due to the influence of the inductor equivalent series resistance.

The simple insertion of an inductive behaviour will directly affect the output reactance value, hence increasing the THD of the system when supplying non-linear loads [6]. To solve this problem, an instantaneous voltage droop is inserted in the virtual impedance, shown on (12), letting the system present a higher resistive behavior at higher frequencies.

$$\upsilon_{ref} = \upsilon_0^* - L_\upsilon \cdot \frac{\omega_p \cdot s}{s+\omega_p} \tag{12}$$

C. Droop Control Loop

The modified Droop control scheme proposed on [1], which has a faster transient response than the classical one, is described on (13) and (14).

$$\omega = \omega^* - m \cdot \tilde{P} - m_d \cdot \frac{\partial \tilde{P}}{\partial t} \tag{13}$$

$$E = E^* - n \cdot Q - n_d \cdot \frac{\partial Q}{\partial t} \tag{14}$$

where

$$\tilde{P} = \frac{\tau^{-1} \cdot s}{(s+\tau^{-1})(s+\omega_c)} \cdot P \tag{15}$$

IV. DROOP CONTROL USING DQ SYNCHRONOUS REFERENCE FRAME

The dq rotating frame transformation is not readily applicable to a single-phase inverter because it needs at least two orthogonal phases. So, in order to use dq frame control techniques, [7] proposes the construction of an imaginary circuit. This dq transformation process turns the time-varying variables of the inverter on DC variables, making the control of the system and the analysis much easier.

A. Imaginary Circuit Construction

The imaginary circuit is constructed based on the real circuit model of the inverter, where the state variables of the imaginary circuit are phase shifted by 90º if compared with the real one [7].

This process of phase shifting can be done by various ways, but the most simple is to apply a delay of a quarter period to the real state variables. On the simulation model presented on this paper, it was used a SOGI-FLL to provide the two orthogonal state variables because it generates them based only on the fundamental frequency, ignoring noises and high order harmonics [8]. The SOGI-FLL can be seen in Fig. 3.

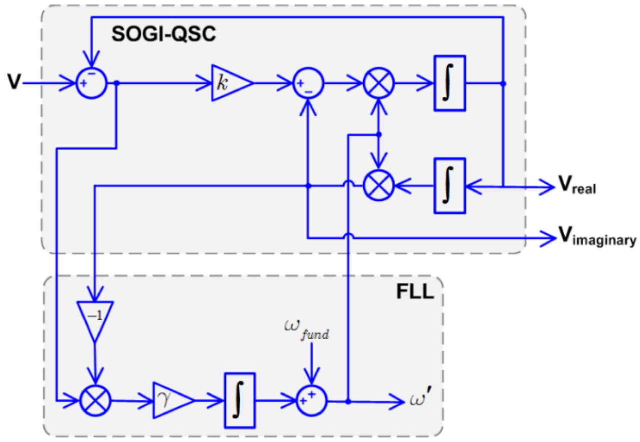

Fig. 3. Block diagram of the SOGI-FLL synchronization system.

B. dq Rotating Reference Frame Inverter Model

The one cycle average model for the real and imaginary circuits is given by:

$$\frac{\partial}{\partial t}\begin{bmatrix}\bar{I}_{LR}\\ \bar{I}_{LI}\end{bmatrix} = -\frac{r_L}{L}\begin{bmatrix}\bar{I}_{LR}\\ \bar{I}_{LI}\end{bmatrix} - \frac{1}{L}\begin{bmatrix}\bar{V}_{CR}\\ \bar{V}_{CI}\end{bmatrix} + \frac{V_{dc}}{L}\begin{bmatrix}\bar{d}_R\\ \bar{d}_I\end{bmatrix} \tag{16}$$

$$\frac{\partial}{\partial t}\begin{bmatrix}\bar{V}_{CR}\\ \bar{V}_{CI}\end{bmatrix} = \frac{1}{C}\begin{bmatrix}\bar{I}_{LR}\\ \bar{I}_{LI}\end{bmatrix} - \frac{1}{ZC}\begin{bmatrix}\bar{V}_{CR}\\ \bar{V}_{CI}\end{bmatrix} \tag{17}$$

where $\bar{I}_{LR}$ and $\bar{I}_{LI}$ are the inductor currents on the real and imaginary circuits and $\bar{V}_{CR}$ and $\bar{V}_{CI}$ the capacitor voltages.

Applying the dq rotating reference frame represented by the transformation matrix T given in (8) to (16) and (17), results in (18) and (19)

$$\frac{\partial}{\partial t}\begin{bmatrix}\bar{I}_d\\ \bar{I}_q\end{bmatrix} = \begin{bmatrix}0 & \omega\\ -\omega & 0\end{bmatrix}\begin{bmatrix}\bar{I}_d\\ \bar{I}_q\end{bmatrix} - \frac{r_L}{L}\begin{bmatrix}\bar{I}_d\\ \bar{I}_q\end{bmatrix} - \frac{1}{L}\begin{bmatrix}\bar{V}_d\\ \bar{V}_q\end{bmatrix} + \frac{V_{dc}}{L}\begin{bmatrix}\bar{d}_d\\ \bar{d}_q\end{bmatrix} \tag{18}$$

$$\frac{\partial}{\partial t}\begin{bmatrix}\bar{V}_d\\ \bar{V}_q\end{bmatrix} = \begin{bmatrix}0 & \omega\\ -\omega & 0\end{bmatrix}\begin{bmatrix}\bar{V}_d\\ \bar{V}_q\end{bmatrix} + \frac{1}{C}\begin{bmatrix}\bar{I}_d\\ \bar{I}_q\end{bmatrix} - \frac{1}{ZC}\begin{bmatrix}\bar{V}_d\\ \bar{V}_q\end{bmatrix} \tag{19}$$

where

$$\begin{bmatrix}0 & \omega\\ -\omega & 0\end{bmatrix} = -T\frac{\partial}{\partial t}(T^{-1}) \tag{20}$$

C. Power Sharing Loop

The dq voltage references are set based on the classical droop method shown on the equations (21), (22) and (23)

$$\omega = \omega^* - m_p \cdot P \tag{21}$$

$$V_d^* = E^* - n_q \cdot Q \tag{22}$$

$$V_q^* = 0 \tag{23}$$

where the reference voltage of the q channel is set to zero, making the output voltage aligned to the d axis on the dq frame and simplifying the analysis of the system.

V. ADAPTIVE DROOP CONTROL

The third droop control technique studied is the one called Adaptive Droop Control proposed by [8]. In this technique the grid parameters are estimated by an algorithm and its output is used on a decoupling method to control of the active and reactive power injections independently.

A. Grid Parameters Estimation

Suppose you have an inverter connected to the grid, as in Fig. 4. The grid parameters estimation technique is based on the voltage and current data obtained on the point of common coupling (PCC) at two operational points to estimate the line impedance Z_g.

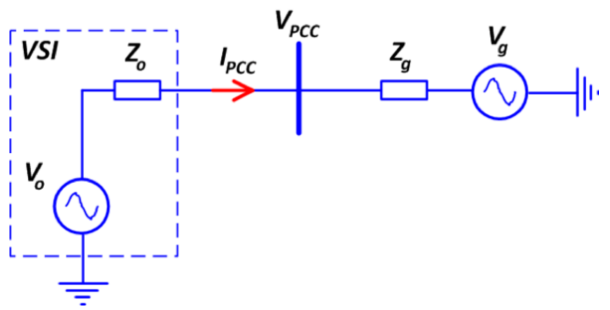

Fig. 4. Schematic diagram for VSI connected to the Grid.

Given the data of the PCC voltage and current on two different operating points, which can be obtained by sampling both at the initial operation of the VSI, the line impedance Z_g is given by (24)

$$\vec{Z}_g = Z_g\theta_g = \frac{\vec{V}_{pcc(2)} - \vec{V}_{pcc(1)}}{\vec{I}_{pcc(2)} - \vec{I}_{pcc(1)}} \tag{24}$$

B. Decoupling Equations

If the variable change given by (25) and (12) is applied to the power flow equations given by (1) and (2), the result is the uncoupled power flow equation given by (27) and (28)

$$P_c = Z_g(P \cdot sin\theta_g - Q \cdot cos\theta_g) \tag{25}$$

$$Q_c = Z_g(P \cdot cos\theta_g - Q \cdot sin\theta_g) \tag{26}$$

$$P_c = E \cdot V \cdot sin\phi \tag{27}$$

$$Q_c = E \cdot V \cdot cos\phi - V^2 \tag{28}$$

Notice now that the powers given by (27) and (28) do not depend on the grid parameters anymore. So, it is possible to control the injection of active and reactive power independently.

C. Droop Functions

So, utilizing equations (25) and (26), results in the following droop functions of this method given by (29) and (30).

$$\phi = -G_p(s) \cdot Z_g\left[(P - P^*) \cdot sin\theta_g - (Q - Q^*) \cdot cos\theta_g\right] \tag{29}$$

$$E = E^* - G_q(s)Z_g\left[(P - P^*)cos\theta_g + (Q - Q^*)sin\theta_g\right] \tag{30}$$

where $G_p(s)$ and $G_q(s)$ can be an integrator, a PI or a PID controller, depending only on the complexity involved in the droop function.

VI. VIRTUAL OSCILLATOR CONTROL

The conventional method for inverters control in micrograds is droop control, which requires no communication and is based on modulating the inverter output such that the frequency and voltage amplitude are inversely proportional to the real and reactive power output, respectively. The droop control is applied in low voltage network, in which the line impedance is resistive, where P-V droop control has been proposed to improve the power sharing and stability.

To overcome shortcomings associated with load-sharing accuracy and system frequency/voltage deviations, recent efforts have focused on the overlay of a communication network between inverters to implement secondary and tertiary controls, which are defined as a hierarchical control structure.

The microgrids cluster systems of the future may need advanced inverters that don’t simply follow what the grid is doing. They should also help to form the grid (grid-forming), by responding to instantaneously to disturbances and working in concern help keep the system stable.

Departing from droop control, a nonlinear control strategy called virtual oscillator control was developed by a NREL team [9]. It is implemented by programming the dynamics of the oscillators onto the inverters’ microcontrollers, and utilizing sinusoidal varying oscillator states to construct modulation control signals [10-12].

The control structure of VOC is shown in Fig. 5. The VOC method has been proven to be independent of load and the number of inverters, requiring no communication and global achieves asymptotic synchronization. However, the duty-ratio of the switching devices are directly controlled by the output of the virtual oscillator. This leads two problems: i) the accurate power sharing is not ensured under mismatch of output impedance; ii) the waveforms of the output voltage is degraded under nonlinear load conditions.

Through comparison between the droop control and VOC, the VOC problem can be improved by using the droop effective control method.

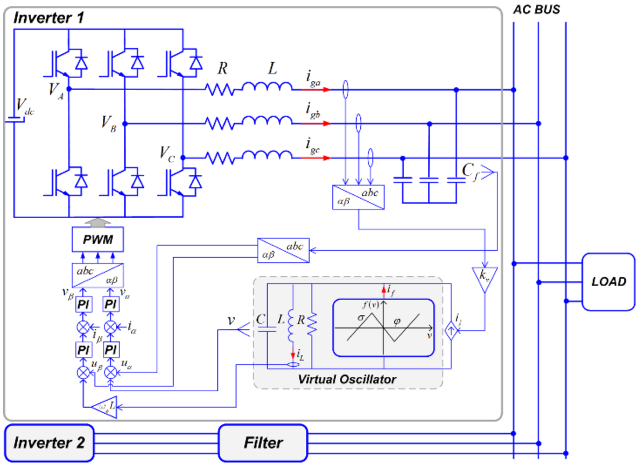

Fig. 5. Control block of VOC inverters in islanding microgrid.

VII. SIMULATION RESULTS

A. Droop Control with Virtual Impedance Loop and Improved Performance

Simulations were developed in the software PSCAD/EMTC in order to test the presented technique. It contains two 1 *kW* Full-Bridge inverters operating at a 20 *kHz* switching frequency and an output voltage of 220 *V* rms. The results are presented for a 1 *kW* load and for a 1 *kVA* non-linear load.

Grid impedances were inserted in the connection of the load to each inverter, one of value $Z_{L1} = 0.434 + j{\cdot}4.8{\cdot}10^{-3}\Omega$ and other of $Z_{L2} = 0.29 + j{\cdot}3.2{\cdot}10^{-3}\Omega$.

1) *Linear Load*: Fig. 6 shows the inverters output currents and the load current.

2) *Non-Linear Load*: The next results were simulated with a non-linear 1000 *VA* load, according to the IEC 62040-3 standards. In Fig. 7, inverter #2 will enter in the grid at time $t = 1s$, so both steady-state and transient can be seen in each frame.

B. dq Rotating Reference Frame Inverter Model

A simulation on the software EMTDC/PSCAD involving both the control and power stage were made to validate the control strategy studied on this chapter. The line impedances used for each inverter were $Z_{L1} = 0.1+j{\cdot}0.25{\cdot}\Omega$ and $Z_{L1} = 0.13 + j{\cdot}0.30\Omega$.

1) *Linear Load*: Fig. 8 shows the load voltage and the output currents of the inverters, respectively, for a linear load of 25Ω.

It can be seen on Fig. 8 that there is a small error on the current sharing between the inverters, this causes a circulating current of nearly 10% of the load current. This shows that can be applied to this system a more efficient droop strategy to eliminate this power sharing error. The circulating current here is defined as the difference between the current of the two inverters.

2) *Non-Linear Load*: Fig. 9 shows the output currents of the inverters for a 1 kVA nonlinear load composed of a full-bridge rectifier and a RC parallel circuit with power factor (PF) equal to 0.70, that was designed based on the IEC 62040-3.

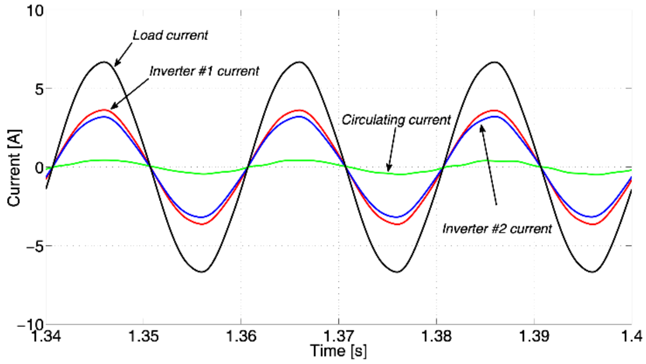

Fig. 6. Details for inverter #1 and #2 output currents, circulating current and load current.

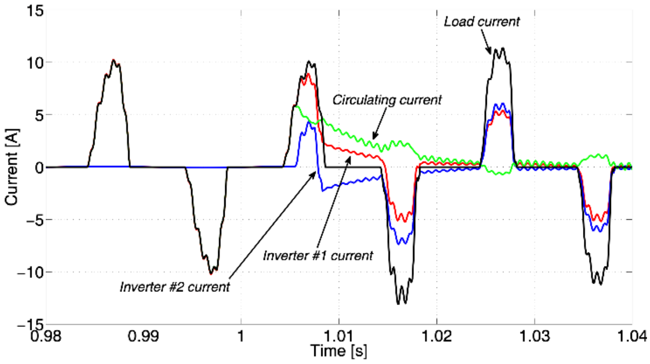

Fig. 7. Non-linear load: Details for inverter #1 and #2 output currents, circulating current and load current.

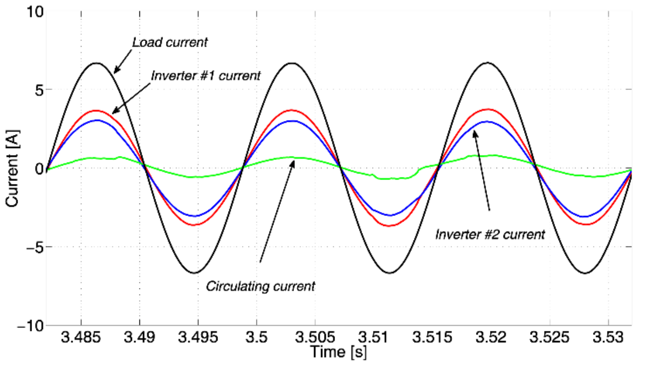

Fig. 8. Details for inverter #1 and #2 output currents, circulating current and load current.

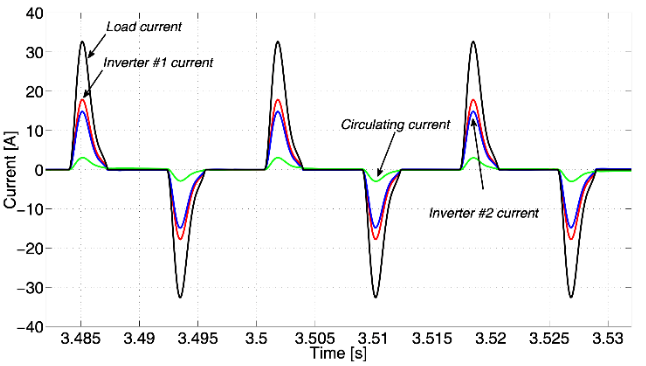

Fig. 9. Non-linear load: Details for inverter #1 and #2 output currents, circulating current and load current.

C. Adaptive Droop Control

The simulation results for this technique were made with two inverters operating in parallel at different locations from a grid of 210 *V rms*. It can be seen the injection of active and reactive power into the grid. Inverter #1 suffers an active power step at t = 4 s and reactive at t = 8 s. With inverter #2 this happens at t = 6 s and t = 10 s, respectively.

VIII. CONCLUSION

A. Droop Control with Virtual Impedance Loop and Improved

As demonstrated on Figs. 6 and 7, the presented control technique may be applied successfully for parallel operation of voltage source inverters. The power sharing accuracy and transient response of the output voltage showed to be valid. Though this, because it possesses a very complicated set of control loops, it is recommended that this technique should only be applied to single-phase inverters.

B. Droop Control Utilizing dq Synchronous Reference Frame

It can be seen on the Figs. 8 and 9 that this method presents a good sharing of the currents, even when a non-linear load is applied. This shows that the dq frame controller applied is effective. Though this, this technique still lacks efficiency on the power sharing loop, with differences between the output currents of nearly 10% of the total load current. Also, because of the simplicity of the model obtained by the dq method, this control scheme is recommended to be applied to three-phase inverters, where there wouldn't even be the need for the imaginary circuit construction, because the three-phase system already can be decomposed on two orthogonal phases by the Clark transform.

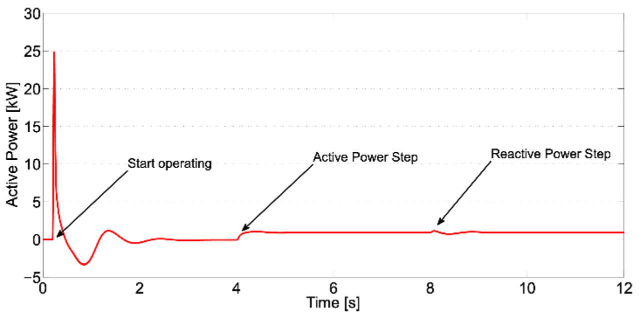

Fig. 10. Inverter #1: Active power.

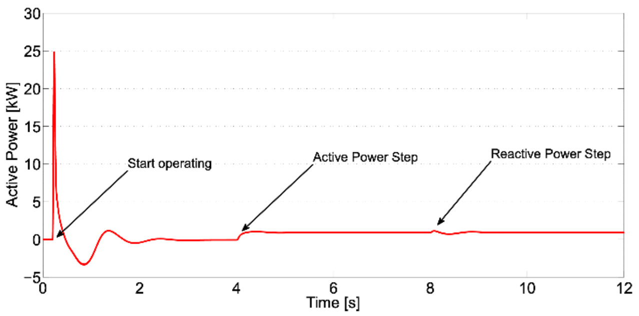

Fig. 11. Inverter #1: Reactive power.

C. Adaptive Droop Control

As seen in Figs. 10 and 11 this control technique can be used to inject active and reactive powers on a grid independently following an arbitrary reference. Though this, the used estimation algorithm needs an independent voltage on the output grid to work, so it can't be applied to UPS systems when sharing common loads.

REFERENCES

[1] J. M. Guerrero, L. G. Vicu˜na, J. Matas et al, "A Wireless Controller to Enhance Dynamic Performance of Parallel Inverters in Distributed Generation Systems," *IEEE Transaction on Power Electronics*, vol. 19, no. 5, pp. 1205-1213, 2004.

[2] J. M. Guerrero, L. G. Vicuña, J. Matas, J. Miret, and M. Castilla, "A high-performance DSP-controller for parallel operation of online UPS systems," *Applied Power Electronics Conference and Exposition*, pp. 463-469, 2004.

[3] J. M. Guerrero, L. Hang and J. Uceda, "Control of Distributed Uninterruptible Power Supply Systems", *IEEE Transaction on Industrial Electronics*, vol. 55, no. 8, pp. 2845-2849, 2008.

[4] R. M. Santos Filho, "Contribuição ao Controle Digital do Paralelismo sem Comunicação de Sistemas de Energia Ininterrupta", *Ph.D. Thesis. Federal University of Minas Gerais*, 2009.

[5] M. C. Chandorkar, D. M. Divan and R. Adapa, "Control of Parallel Inverters in Stand-Alone AC Supply Systems," *IEEE Transactions on Industry Application*, vol. 29, no. 1, pp. 136-143, 1993.

[6] J. M. Guerrero, L. G. de Vicuña, J. Matas, J. Miret and M. Castilla, "Output Impedance Design of Parallel-Connected UPS Inverters with Wireless Load-Sharing Control," *IEEE Transactions on Industrial Electronics*, vol. 52, no. 4, pp. 1126-1135, 2005.

[7] S. Golestan, M. Joorabian, H. Rastegar, A. Roshan and J. M. Guerrero, "Droop Based Control of Parallel-Connected Single-Phase Inverters in dq Rotating Frame," *ICIT 2009, International Conference on Industrial Technology*, pp. 1-6, 2009.

[8] J. C. Vasquez Quintero, "Decentralized Control Techniques Applied to Electric Power Distributed Generation in Microgrids", *Ph.D. Thesis. Universitat Politécnica de Catalunya*, 2009.

[9] B. B. Johnson, et al. "Synthesizing Virtual Oscillators to Control Islanded Inverters," *IEEE Transactions on Power Electronics*, vol. 31, no. 8, pp. 6002-6015, 2016.

[10] B. B. Johnson, et al. "Oscillator-based inverter control for islanded three-phase microgrids," *IEEE Journal of Photovoltaics*, vol. 4, no. 1, pp. 387-395, 2014.

[11] B. B. Johnson, et al. "Synchronization of parallel single-phase inverters with virtual oscillator control," *IEEE Transactions on Power Electronics*, vol. 29, no. 11, pp. 6124-6138, 2014.

[12] S. V. Dhople, B. B. Johnson and A. O. Hamadeh, "Virtual Oscillator Control for voltage source inverters," *51st Annual Allerton Conference on Communication, Control, and Computing*, pp. 1359-1363, 2013.